DIGITAL TOPOGRAPHIC MODELS OF TITAN PRODUCED BY RADAR STEREOGRAMMETRY WITH A RIGOROUS SENSOR MODEL. R. L. Kirk[1], E. Howington-Kraus[1], B. W. Stiles[2], S. Hensley[2], and the Cassini RADAR Team, [1]U.S. Geological Survey, Astrogeology Program, Flagstaff, AZ 86001 (rkirk@usgs.gov), [2]Jet Propulsion Laboratory, Pasadena, CA 91109.

Introduction: The Cassini RADAR instrument [1] provides the highest resolution images of Titan's surface, apart from local coverage of the Huygens landing site by the DISR cameras. RADAR has imaged approximately 22% of Titan's surface with its synthetic aperture radar (SAR) mode so far, at resolutions from about 0.3 to 1.5 km. Beginning in late 2006, most new SAR image strips partly overlapped one or more earlier images. By the end of 2007, more than 20 image pairs covering more than 1% of Titan were available. These stereo pairs encode information about the topographic relief of Titan's surface in the parallax distortions that occur when the surface is viewed from different directions. It has thus become possible, by matching surface features (each a few times the image resolution in horizontal extent) in the paired images and then using radar stereogrammetry to calculate the three-dimensional surface coordinates of these features, and thus to make digital topographic models (DTMs) of selected areas of Titan with a horizontal resolution of a few km and a vertical precision of a few hundred meters. Such resolution compares usefully with those of other topographic datasets, such as altimetry [2] (tens of km), "SAR topography" [3] (~10 km), and radarclinometry/shape-from-shading [4, 5] (the image resolution, ~1 km).

We previously described the geomorphology of the first four RADAR stereopairs of Titan and our preliminary attempts to derive topographic information [6]. Similar methods were subsequently applied [7] to additional images covering terrain near Titan's large north polar seas [8]. In this early work, corresponding features in the paired images were located either by interactive spot measurements or by automated image matching techniques. In either case, relative elevations were then calculated by an approximation, in which the incidence angles of the two images are used to calculate a proportionality between parallax displacement and relative elevation [9]. By comparing our results with SAR topography, we showed [7] that accurate relative (but not absolute) heights can be obtained where the two images have similar look directions and different incidence angles, but that where the images differ more in look direction than in incidence angle, results become unreliable.

In this abstract, we describe work at the USGS to incorporate a physically rigorous model of the geometry of RADAR image formation (called a "sensor model") into a commercial digital photogrammetric workstation and show our first results with this approach, which lets us calculate absolute heights and parallax-corrected horizontal coordinates of the features mapped. We note that one of our coauthors (Hensley), who had adapted his Magellan SAR image-matching software to work with Cassini data [6], has independently developed a rigorous Cassini sensor model. The resulting data products should be of similar quality to those described here, with similar scientific applications.

Methodology: To perform stereogrammetric analysis of Cassini SAR data, as well as of a wide variety of other planetary images, the USGS uses the software package SOCET SET ® available from BAE Systems [10]. The in-house cartographic software package ISIS [11] is used to prepare the images and supporting metadata in formats that the commercial software can understand. SOCET SET provides many useful capabilities, including a versatile automated image matching algorithm (Automatic Terrain Extraction, or ATE) and the ability to overlay the resulting DTM data on the images in a stereoscopic video display in order to validate the results of ATE and edit them where necessary, or even to create DTMs manually (Interactive Terrain Editing, or ITE). The stereo display can be used to overlay other data such as SAR topography on the images, and to measure the locations of individual features, which can then be used to improve the alignment of the images with one another and with ground control (if available)

All of these functions require a sensor model to calculate the image pixel that corresponds to a given ground location in latitude, longitude, and elevation, or the reverse. Models for some sensors are available from BAE, but the Cassini RADAR has unique aspects that required us to develop our own sensor model by using the SOCET Developer's Toolkit (Devkit), as we had previously done for Magellan [12].

The fundamental observables for SAR are the range and Doppler shift at which a feature is observed at a given time. Given the position and velocity of the spacecraft at that time, calculating the range and Doppler shift is a straightforward exercise in geometry. The main complication in sensor modeling for both Magellan and Cassini is that the images (Basic Image Data Records or BIDRs [13]) have been prepared in map projection. That is, nominal ground coordinates corresponding to a given range-Doppler observation were computed based on a particular surface model (for Titan, a 2575 km sphere) and a particular spacecraft trajectory (for Cassini, stored in the Burst Ordered Data Product or BODP [14] that accompanies a given BIDR) and these nominal coordinates were used to locate the point within the map. It is necessary to reverse this calculation and reconstruct the observed range-Doppler coordinates of a given pixel before proceeding to calculate the "true" ground coordinates. These will differ from the nominal coordinates because the elevation of the point is accounted for, and possibly also because the spacecraft trajectory has been adjusted to provide better registration with other datasets. This adjusted trajectory must be kept carefully distinct from the nominal trajectory.

The other significant complication to the sensor model arises from the question: at what time should the range and Doppler of a given image point be calculated? The resulting "true" ground coordinate is insensitive to this choice, but the preferred time is that of the radar burst that illuminated the area most nearly centered on the particular point. The required information (coordinates of an ellipse approximating the illuminated area for each burst) is available in the tabular BODP. We rasterize these data to create a mask image that indicates the burst(s) in which each ground point was observed; this approach is simpler than constructing a database of polygons outlining the bursts as we did for Magellan, but is only feasible because the Cassini images are smaller than typical Magellan products. The mask image is in the same projected coordinates as the BIDR, but has four times coarser spatial resolution. The mask image is produced as part of the ISIS pre-processing needed in order to import a given BIDR into SOCET SET; other preparatory steps include formatting the BIDR so it can be read by SOCET SET, and extracting the trajectory data from the BODP. BIDR products released to the PDS so far contain subtle geometric distortions introduced during radiometric correction of the images. We make use of specially processed BIDRs from which these distortions have been eliminated. A full set of such reprocessed BIDRs will be delivered to the PDS by mid-2008.

First Results: We have focused initially on the overlap between the T25 and T28 radar swaths near the north pole because (a) misalignment of these images caused by errors in the model of Titan's spin [14] is minimal, (b) the apparent relief in this area is dramatic compared to most other pairs, and (c) the topography and slopes associated with the large "seas" in this area are of tremendous interest for understanding Titan's organic inventory [16] and methane equivalent of a hydrologic cycle [17, 18, 19]. We first used ITE to collect an elevation profile along the track of the T25

SAR topography, finding that the two sets of elevations differed by 50 m or less in most places, including toward the east end of the pair where results obtained by simple parallax-height scaling were in error by as much as 50%. This is excellent agreement, considering that the estimated vertical precision of the SAR topography is 30–70 m and that 50 m elevation difference in stereo corresponds to a typical parallax of only ~100 m. The actual resolution of the images, based on the size of coherent "speckle" is ~1000 m for T25, and ~500 m for T28, indicating that sub-resolution (and, indeed, sub-pixel) matching has probably been achieved.

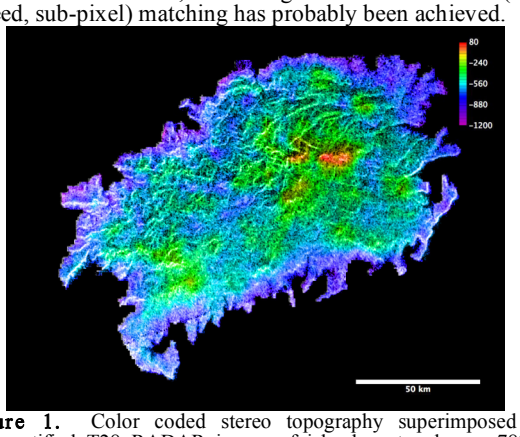

Figure 1. Color coded stereo topography superimposed on orthorectified T28 RADAR image of island centered near 78° N 312° W. Equirectangular projection with center latitude 79° N, 175 m/pixel, north at top. Elevations are referenced to 2575 km radius.

DTM production with ATE requires experimentation to adjust the parameters of the matching algorithm for each new dataset. We therefore began by mapping a limited area, the 90x150 km island centered near 78° N 312° W (Fig. 1). Success with ATE was greatly improved by first collecting a sparse "seed" DTM interactively, which we had previously found to be helpful with Magellan images [12]. Some editing of the ATE result to remove localized artifacts was also necessary. The resulting DTM corresponds well to the morphology revealed in the images, and appears to resolve features at least as small as 5 km horizontally. Elevations along the shoreline, which ought to be constant, are consistent within a few hundred meters, with the greatest variation occurring where the image shows steep coastal scarps that the DTM is clearly unable to resolve. Total relief from coast to interior is ~1200 m over a distance of 40 km (for a mean slope of 1.5°); the RMS (root-mean-squared) slope over short distances is ~3°. The relief of this rugged-appearing island is thus quite subtle (Fig. 2).

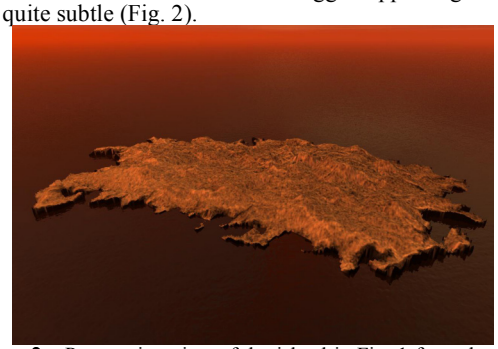

Figure 2. Perspective view of the island in Fig. 1 from the southeast with vertical exaggeration 10. False color and simulated "liquid" surface are intended to suggest Titan conditions.

SAR topography heights in this area are below the corresponding DTM heights and even below the coastline despite the good agreement of the two datasets elsewhere. We believe the discrepancy results from the proximity of the SAR topography trace to the coast. Because the SAR topography is obtained by comparing backscatter intensities on the fringes of two overlapping radar beams [3], the result may well be biased when the overlap area contains an extremely high contrast feature such as the coastline. We also compared the stereo DTM to topographic profiles obtained by radarclinometry (RC). Good agreement was obtained along a profile through the highest peak in the eastern part of the island when a cotangent-of-incidence backscatter function was used [5]. RC profiles across the western part of the island differed radically from the DTM, however, showing a peak 2500 m above the coast whereas the DTM indicates a plateau <500-m high. The results can be reconciled if the very bright area along the south coast of the island, which the RC algorithm interprets as a steep slope, is instead a region of intrinsically stronger backscatter than the rest of the island. There is an obvious lesson that RC results must be viewed with initial skepticism and care taken to rule out the presence of even subtle backscatter variations that might distort the profile. We note, however, that the largest elevations obtained for RC profiles Titan's mountains are less than 2000 m, thus excluding errors of the magnitude seen here [4].

Future Work: We are currently producing a DTM covering as much of the land area of the T25-T28 overlap as possible. Features are visible in the "sea" to the north of the island shown here (which could potentially be marshy rather than liquid-covered) and possibly in other, darker parts of the seas as well. We will map the bathymetry of these areas if possible. We will next collect a DTM from the T25-T29 pair, which covers a large additional area of the northern seas as well as a strip extending to the equator. The landforms along much of this strip are less dramatic than near the pole, but the higher resolution of the closest-approach portions of the images may reveal more subtle relief. The results may guide planning for the collection of additional long-strip stereopairs during Cassini's second extended mission. We will show these products in our LPSC presentation.

Further progress with stereo topographic mapping will come after the full set of RADAR BIDRs have been reprocessed based on the improved model of Titan's rotation [15]. This should bring the full set of images into alignment at ~1 km accuracy or better, and refining the ephemerides for the flybys by bundle adjustment should further reduce the discrepancies, allowing us to produce a complete set of stereo DTMs with absolute elevations consistent with one another as well as with the SAR topography and altimetry profiles. This dataset will allow us and others to begin addressing a wide variety of intriguing topics such as the height differences and slopes driving subsurface [17] and surface [18, 19] flow of methane, the interaction of dunes with topography [20], and the extent and nature of cryovolcanism [21].

References: [1] Elachi, C. et al. (2004) *Space Sci. Rev., 115*, 71. [2] Johnson, W.T.K. et al. (2007) Workshop on Ices, Oceans, and Fire, LPI Contribution 1357, 70. [3] Stiles, B.W. et al. (2006) *AAS Bull., 38*, 57.07. [4] Radebaugh, J. et al. (2007) *Icarus*, doi:10.1016/j.icarus.2007. 06.020. [5] Kirk, R.L. et al. (2007) ISPRS Working Group IV/7 Workshop, available online at http://www.dlr.de/pf/Portaldata/6/Resources/dokumente/isprs_2007/Kirk_3__ISPRS_2007.pdf. [6] Kirk, R.L. et al. (2007) *LPS XXXVIII*, 1427. [7] Kirk, R.L. et al. (2007) *Eos, 88*(52), P22B-01. [8] Mitchell, K.L. et al. (2007) *Eos, 88*(52), P23B-1349. [9] Plaut, J.J. (1993) in *Guide to Magellan Image Interpretation*, JPL Pub. 932-24, 33. [10] Miller, S.B., and A.S. Walker (1993) *ACSM/ASPRS Annual Conv., 3*, 256; (1995) *Z. Phot. Fern. 63*, 4. [11] Eliason, E. (1997) *LPS XXVIII*, 331; Gaddis, L.R. et al. (1997) *LPS XXVIII*, 387; Torson, J., and K. Becker, (1997) *LPS XXVIII*, 1443. [12] Howington-Kraus, E. et al. (2000) *LPS, XXXI*, 2061; (2002) *LPS, XXXIII*, 1986. [13] Stiles, B. (2005) Cassini Radar BIDR SIS, JPL D-27889, v. 1.3. [14] Stiles, B. (2005) Cassini Radar BODP SIS, JPL D-27891, v. 1.4. [15] Stiles, B.W. et al. (2008) *Astron. J.*, submitted. [16] Lorenz, R.D. et al. (2008) *GRL*, in press. [17] Aharonson, O. et al. (2007) *Eos*, 88(52) P23B-1350. [18] Perron, J.T. et al. (2006) *JGR, 111*(E11), E11001. [19] Burr, D.M. et al. (2006) *Icarus, 88*(1), 235. [20] Radebaugh, J. et al. (2008) *Icarus*, in press. [21] Lopes, R.M.C. et al. (2007) *Icarus, 187*, 395.